

## 6.8 THE EFFECTS OF DIABATIC REDISTRIBUTION OF POTENTIAL VORTICITY ON COLD FRONTAL RAINBANDS AND COLD FRONT PROPAGATION

Heather Dawn Reeves \*and Gary M. Lackmann  
North Carolina State University  
Raleigh, NC

### 1. Introduction

The purpose of this research is to investigate whether diabatic potential vorticity (PV) redistribution affects cold frontal propagation.

Raymond and Jiang (1990) found that when latent heating and a positive PV anomaly are vertically aligned in a sheared environment, positive PV is redistributed downwind of the current anomaly. This implies that PV anomalies are able to propagate independent of the advecting wind. In the vicinity of a baroclinic zone, PV anomalies could, in principle, propagate into the prefrontal zone (PFZ), given favorable shear and diabatic heating profiles. Increased PV in the PFZ is an indication that a) a cyclonic wind shift is introduced in the PFZ while the wind shift across the FZ is reduced, and b) lifting associated with PV-forced isentropic ascent (Raymond and Jiang 1990) can induce precipitation in the PFZ leading to an increased temperature contrast in the PFZ and a reduced temperature contrast across the FZ.

*The hypothesis of this research is that modification of the PFZ can lead to frontal acceleration by introducing front-like characteristics ahead of the actual front while reducing temperature and wind shift contrasts across the FZ.*

Cold frontal weather, in particular precipitation, has been targeted as an area where numerical weather prediction models fail to perform well due to the need for parameterization of sub-grid scale processes (Wang and Seaman 1997). Assuming the hypothesis is correct, the failure of a model to accurately repre-

sent precipitation could lead to errors in forecasts of cold-frontal position.

The goals of this study are to assess the dependency of the intensity and positioning of cold frontal PV anomalies on latent heating and convection and to evaluate the connection between PV redistribution and frontal propagation.

### 2. Case Study

A cold front with vertically aligned latent heating and a positive PV anomaly located in the FZ was examined to see if diabatic PV redistribution occurred concurrent with frontal acceleration. This cold front took place on 29-30 Jan. 2001. It started life as a stationary front in central Texas, along the eastern edge of a small high pressure system at 18UTC on 28 Jan 2001. Between 06 UTC and 09 UTC, a closed surface low developed on the north end of the front and the front began to propagate eastward. Figure 1 shows the speed of the front from 00 UTC to 21 UTC, according to surface observations. From 06 UTC to 12 UTC, the front experienced an acceleration from about 8m/s to just over 14m/s. This acceleration occurred in conjunction with the precipitation band moving from being completely behind the front to portions of the precipitation band being in the PFZ.

Eta model analyses obtained from Unidata Local Data Manager (40km horizontal grid spacing, 25hPa vertical spacing) were used to budget the PV field modified from Lackmann (2002) (adapted from Cammas et al. 1994 and Raymond 1992).

---

\*Corresponding author address: Marine, Earth and Atmospheric Sciences North Carolina State University Box 8208 Raleigh, NC 27695-8208 email: hdreeves@unity.ncsu.edu

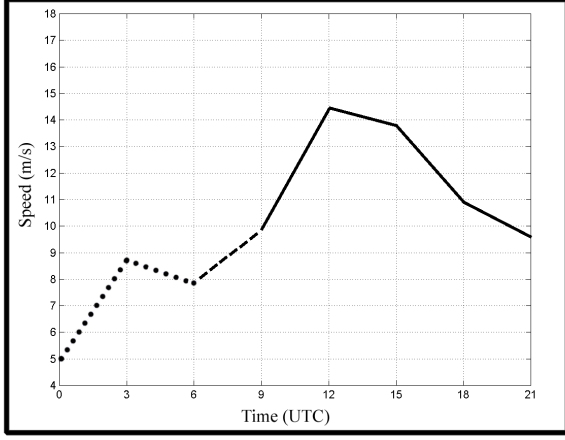


Figure 1: Frontal speed as a function of time for 29 Jan 2001 (along 32°N). Dotted line represents times when no precipitation was in the prefrontal zone, solid line represents times when precipitation was in the prefrontal zone, the dashed line represents the transition time. These speeds are derived from 3 hourly surface observation analyses.

$$\frac{\partial P}{\partial t} = \underbrace{-\vec{\nabla}_p \cdot (P\vec{V}_h)}_A - \underbrace{\frac{\partial}{\partial p}(P\omega)}_B - \underbrace{g\vec{\nabla}_3 \cdot \vec{Y}}_C, \quad (1)$$

where  $P$  is Ertel's potential vorticity,

$$P = g(f\hat{k} + \vec{\nabla}_3 \times \vec{V}_h) \cdot \vec{\nabla}_3 \theta, \quad (2)$$

and  $\vec{Y}$  is the non-advective potential vorticity flux vector, which can be approximated by

$$\vec{Y} = -\frac{d\theta}{dt} \left( f\hat{k} + \vec{\nabla}_3 \times \vec{V}_h \right). \quad (3)$$

Frictional effects were neglected in the calculation of  $\vec{Y}$  in order to isolate the effects of diabatic heating on PV production.

The latent heating rate  $\left(\frac{d\theta}{dt}\right)$  was approximated using the following equation (after Emanuel et al. 1987):

$$\frac{d\theta}{dt} = \omega \left( \frac{\partial \theta}{\partial p} - \frac{\Gamma_m}{\Gamma_d} \frac{\theta}{\theta_e} \frac{\partial \theta_e}{\partial p} \right). \quad (4)$$

In the above equations,  $\vec{\nabla}_p$  is the horizontal gradient operator on an isobaric surface,  $\vec{V}_h$  is the horizontal wind vector,  $\vec{\nabla}_3 = \vec{\nabla}_p - \hat{k} \frac{\partial}{\partial p}$ ,  $g$  is gravitational acceleration,  $f$  is the Coriolis parameter,  $\theta$  is

potential temperature,  $\Gamma_m$  and  $\Gamma_d$  are the moist and dry adiabatic lapse rates, and  $\theta_e$  is equivalent potential temperature. In equation (1), term A is the horizontal advective flux divergence, term B is the vertical flux divergence, and term C is the diabatic PV tendency term.

At 12UTC on 29 Jan. 2001 (the time the front moved the fastest), the PV budget reveals there were positive, diabatic PV tendencies in the PFZ (see Figure 2) between 32° and 34°N. This is an indication that the processes outlined above were active in the PFZ at this time and could have been responsible for the frontal acceleration that occurred between 06 UTC and 12 UTC.

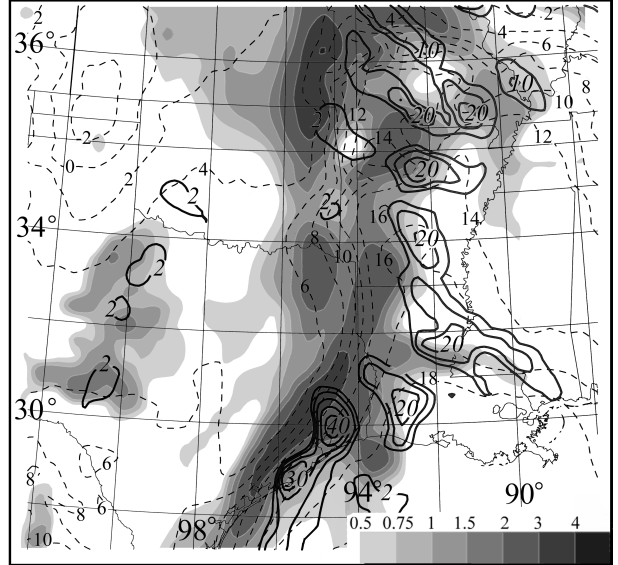


Figure 2: Potential vorticity layer averaged from 925-900 hPa (shaded - see legend in figure box), wet-bulb potential temperature at 975 hPa (dashed - contoured every 2°C), and positive, diabatic PV tendencies at 925 hPa (solid lines - contour interval starts at  $2 \times 10^{-5}$  PVU  $s^{-1}$ , then in intervals of  $10 \times 10^{-5}$  PVU  $s^{-1}$ , only inner contour values are provided in figure) at 12 UTC on 29 Jan 2001. (1 PVU  $\equiv 10^{-6} m^2 s^{-1} K kg^{-1}$ )

### 3. Preliminary Results

In order to test the hypothesis, numerical simulations using the fifth-generation Pennsylvania State University-National Center for Atmospheric Research Mesoscale Model (MM5) (Dudhia 1993) were performed. Forty-five sigma levels on a two-domain system were used.

The outer domain had a horizontal resolution of 45km while the inner domain, which contained all frontal activity, had a horizontal resolution of 15km. Two-way interaction was allowed between the domains. The model physics used are: simple ice cloud physics (Lin et. al. 1983), Kain-Fritsch convective parameterization scheme, and MRF planetary-boundary layer. Model initial conditions were taken from the Eta 40 km grid spacing analyses. The simulation was initiated at 18 UTC 28 Jan 2001 and ran until 00 UTC 30 Jan 2001. There are some minor differences between the full-physics simulation (the control run) and Eta model data. The temperature gradient across the Eta model analysis is not as tight as that across the control run, and the pressure centers in the control run are not as deep as those in the Eta model analysis. This was not deemed to be an issue, however, since the processes involving PV redistribution were still present.

The control run is compared to a second simulation neglecting latent heating and convective motions (fake-dry run). When effects of latent heating are “turned off,” evaporative cooling cannot influence the temperature gradient across the FZ and latent heating cannot induce cyclonic shear in the PFZ. Therefore, the processes at play which are presumed to lead to frontal acceleration will not exist. Should the front move more slowly in the fake-dry run, some support will be gained for the hypothesis.

Preliminary results from the simulations support the hypothesis. Figure 3 shows the speed of the front for both the control run and the fake-dry run from 00 UTC to 20 UTC 29 Jan 2001. (Frontal positions were derived using 1000 hPa temperature, wind shift and sea-level pressure analyses.) Clearly, the fake-dry run front does not move as fast as the front in the control run.

Should the disparity in speed be the result of different latent heating rates between the two simulations, the resulting PV fields should manifest these differences. Figure 4 shows PV (shaded), wet-bulb potential temperature (dashed contours) and wind barbs (m/s) at 13 UTC on 29 Jan 2001 (19 hours into the simulation) for the control run (a) and the fake-dry run (b). Notice that some positive PV values exist in the PFZ and are accompanied by a healthy low-level jet (LLJ)( $30\text{ms}^{-1}$  maximum) in the con-

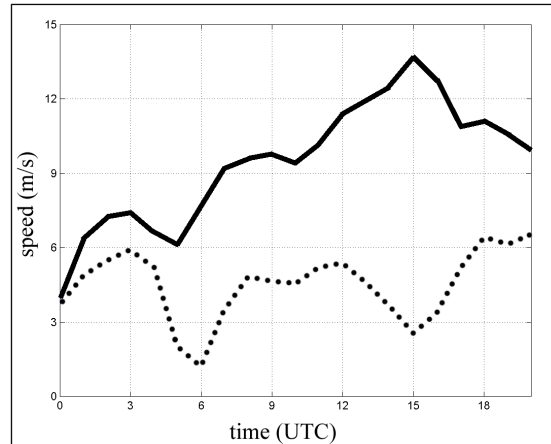


Figure 3: Frontal speed as a function of time for 29 Jan 2001 control run (thick, solid line) vs. the fake-dry run (dotted line) averaged from  $31^{\circ}$  to  $34^{\circ}\text{N}$ .

trol run. Conversely, the PV anomaly in the fake-dry run is considerably weaker (maximum frontal PV in control = 4PVU, maximum frontal PV in fake-dry = 0.75PVU) and is behind the frontal zone. Furthermore, the LLJ is much weaker in the fake-dry simulation. This is in keeping with a previous PV study which suggests cold-frontal PV anomalies may contribute up to as much as 40% of the total low-level jet (Lackmann 2002).

It is possible that a feedback mechanism developed in the control run that did not develop in the fake-dry run. The stronger LLJ in the control run likely led to greater moisture transport. This is evinced in the model precipitation fields which show that control run precipitation fields are heavier and more cellular than fake-dry precipitation fields (not shown).

## 4. Conclusions

Potential vorticity anomalies situated parallel to cold fronts can act to alter the prefrontal environment in such a way that front-like characteristics are introduced in the PFZ, while contrasts in temperature and wind shift are reduced across the FZ. This process is hypothesized to lead to frontal acceleration. A case study of a cold front which propagated west-to-east along the southern Great Plains is presented. This front appears to have accelerated due to the above process. Numerical simulations help to support this

claim. Further sensitivity tests isolating the effects of condensational heating vs. evaporational cooling have yet to be performed. It is possible that other processes not yet accounted for are the true cause of frontal acceleration. These other candidates will be explored in future simulations.

## 5. Acknowledgments

The authors wish to express special thanks to the National Science Foundation for funding this research (Grant # ATM-0079425), the Unidata program for providing observational and Eta model data, NCAR/MMM for providing the MM5 model, and Ms. Margaret Puryear for assisting with the data.

## 6. References

- Bergeron, T., 1937: On the physics of fronts. *Bull. Amer. Meteor. Soc.*, **18**, 265-275.
- Cammas, J.P., D. Keyser, G.M. Lackmann, and J. Molinari, 1994: Diabatic redistribution of potential vorticity accompanying the development of an outflow jet within a strong extratropical cyclone. *Proc. Int. Symp. on the Life Cycles of Extratropical Cyclones*, Vol. III, Bergen Norway, Geophysical Institute, University of Bergen. 403-409.
- Dudhia, J., 1993: A nonhydrostatic version of the Penn. State-NCAR Mesoscale Model: Validation tests and simulations of an Atlantic cyclone and cold front. *Mon. Wea. Rev.*, **117**, 1493-1513.
- Emanuel, K.A., M. Fantini, and A.J. Thorpe, 1987: Baroclinic instability in an environment of small stability to slantwise moist convection. Part I: Two-dimensional models. *J. Atmos. Sci.*, **44**, 1559-1573.
- Lackmann, G.M., 2002: Cold-frontal potential vorticity maxima, the low-level jet, and moisture transport in extratropical cyclones. *Mon. Wea. Rev.*, **130**, 59-74.
- Lin, Y.L., R.D. Farley, and H.D. Orville, 1983: Bulk parameterization of the snow field in a cloud model. *J. Climate Appl. Meteor.*, **22**, 1065-1092.
- Raymond, D.J., 1992: Nonlinear balance and potential vorticity thinking at large Rossby number. *Quart. J. Roy. Meteor. Soc.*, **118**, 987-1015.
- , and H. Jiang, 1990: A theory for long-lived mesoscale convective systems, *J. Atmos. Sci.*, **47**, 3067-3077.
- Wang, W. and N.L. Seaman, 1997: A comparison study of convective parameterization schemes in a mesoscale model. *Mon. Wea. Rev.*, **125**, 252-278.

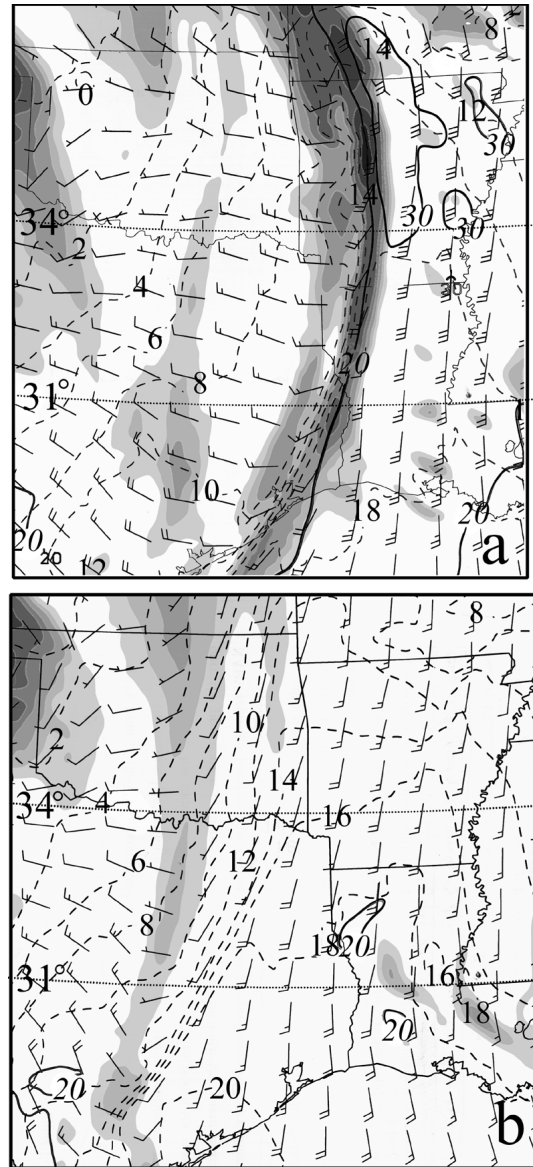


Figure 4: Potential vorticity layer averaged from 950-900 hPa (PVU, shaded, see legend in Figure 2), wet-bulb potential temperature at 1000 hPa (dashed - every  $2^{\circ}\text{C}$ ), wind barbs (1 full barb =  $10\text{m s}^{-1}$ ,  $\frac{1}{2}$  barb =  $5\text{m s}^{-1}$ ), and wind contours ( $20\text{m s}^{-1}$  and  $30\text{m s}^{-1}$ ) at 13 UTC on 29 Jan 2001 for the control run (a) and the fake-dry run (b).